Green Chemistry

PAPER

Cite this: *Green Chem.*, 2015, **17**, 4991

Reversible crosslinking of lignin *via* the furan–maleimide Diels–Alder reaction†

Antoine Duval,[a,b] Heiko Lange,[b] Martin Lawoko*[a] and Claudia Crestini*[b]

Received 14th June 2015,
Accepted 31st July 2015

DOI: 10.1039/c5gc01319d

www.rsc.org/greenchem

Two distinct functionalization schemes for Kraft lignin (KL) were developed to selectively incorporate furan and/or maleimide motifs as chain ends. The incorporation of furan functionalities was carried out by the selective and quantitative reaction of the lignin's phenolic OH groups with furfuryl glycidyl ether (FGE). Maleimide groups were introduced by esterifying the lignin's aliphatic and phenolic OH groups with 6 maleimidohexanoic acid (6-MHA), offering a high loading despite a somewhat incomplete conversion. Furan- and maleimide-functionalized lignins were subsequently combined to generate crosslinking *via* the Diels–Alder (DA) [4 + 2] cycloaddition reaction. The formation of the DA adduct was confirmed by ^{1}H NMR. Under appropriate conditions, the formation of a gel was apparent, which turned back into the liquid state after performing the corresponding retro-DA reaction upon heating to 120 °C. This study reveals the significant versatility and potential of the developed strategy for the utilization of lignin-based recyclable networks.

Introduction

Lignin is a widely abundant biopolymer, naturally synthesized in vascular plants by the polymerization of phenylpropane units. In softwood, the lignin content can reach 30% by weight.[1] It is structurally a rather complex polyphenol, of large variety and diversity, originating from the fact that different wood species and variable extraction processes impose different structural characteristics on lignin.

Paper pulp processes, among which the Kraft process predominates,[2] produce industrially large amounts of lignin, estimated to be about 70 Mt per year.[3] Nevertheless, most of it gets burnt in plants to produce energy, thus limiting the amount of commercially available Kraft lignin (KL) to only 100 000 t per year.[4] However, the interest in lignin among researchers in chemistry and polymer science has been growing rapidly in the past few years, motivated by the need for alternatives to petroleum-based aromatic compounds and by the development of biorefinery processes expected to significantly increase their commercial availability. Progress in controlled lignin depolymerization,[5,6] involving the development of specific catalysts,[7–9] could for example allow the production of phenol and its derivatives.

The direct use of lignin as a polymer is made difficult by its complex and variable macromolecular structure. Despite the huge efforts devoted to its structural characterization during the last few decades, a clear idea of its molecular structure emerged only in the last few years with the development of advanced heteronuclear 2D NMR techniques. More specifically, the characterization and quantitative evaluation of the different lignin interunit bondings, coupled with wet chemistry methods, recently allowed researchers to elucidate unprecedented structural details and to obtain a detailed map of its different functionalities.[10,11] Furthermore, recent advances in the isolation of low polydispersity lignin fractions, either by membrane filtration[12–14] or solvent fractionation,[15,16] have contributed to enhance its potential use.

As a multifunctional polymer displaying many aliphatic and phenolic OH groups, lignin actually offers plenty of opportunities for functionalization.[17] The control of the lignin multifunctional character constitutes a key step to achieve upgrade and valorization, and remains today a challenge contributing to the difficulty of developing lignin-based materials. The multifunctional character of lignin has naturally been exploited to form polymer networks, in an attempt to produce bio-based resins. The crosslinking of lignins with aldehydes, diacids or diisocyanates has for example been reported,[17] as well as radical polymerization.[18] Lignin-based fibers have also been generated, *e.g.* by electrospinning of lignins.[19] Nevertheless, all these materials contain either chemical bonds that are permanent, which implies for instance that the materials cannot be

[a]*Wallenberg Wood Science Center (WWSC), Department of Fiber and Polymer Technology, KTH Royal Institute of Technology, SE-100 44 Stockholm, Sweden. E-mail: lawoko@kth.se; Tel: +46 8 7908047*

[b]*Department of Chemical Sciences and Technologies, University of Rome 'Tor Vergata', Via della Ricerca Scientifica 1, 00133 Rome, Italy. E-mail: crestini@stc.uniroma2.it; Tel: +39 067259 4734*

†Electronic supplementary information (ESI) available. See DOI: 10.1039/c5gc01319d

recycled or used in more sophisticated applications that require, for example, reversible matrix-generation, or no real chemical bonds at all, a fact that comes with other disadvantages. An important field of research in polymer materials is thus concerned with the establishment of reversible crosslinking capabilities,[20,21] which opens a route toward obtaining recyclable networks[22] and self-healing materials.[23–25] Materials science applications come into play, in which temporarily switching from a liquid to a solid state is desirable, *i.e.*, solidifiable liquids, *e.g.*, for use in technical devices that are in principle flexible, but carrying reversible stiffness, and that are thus able to reach locations difficult to access with stiff devices; applications range from stabilizing cavities in crashed houses in disaster settings to stabilizing smaller cavities emerging during natural aging of materials, *e.g.*, aging of wood. The combination of a temporary crosslinking realized on a lignin-backbone allows the generation of novel polymer-based adhesives and coatings exhibiting a double, *i.e.*, a temporary and a permanent curing system: such functional polymers can be temporarily fixed for trial purposes or accuracy checks before a 'classical', permanent curing system is activated.[26,27]

The Diels–Alder (DA) [4 + 2] cycloaddition between furan and maleimide moieties, which respectively act as a diene and a dienophile, represents, among others, an interesting tool to generate bonds in a reversible fashion.[28] It presents several advantages, such as the low temperatures required to perform the forward and retro reactions, at 60–70 and 110–120 °C, respectively, which are compatible with the thermal stability of most polymers. In addition, a wide range of furan monomers can be prepared from furfural and hydroxymethylfurfural, respectively, obtained from bio-based polymers (C5 or C6 sugars in polysaccharides).[29]

In this study, we aimed at creating a novel temperature responsive material combining the multifunctional character of lignin with the attractive features of the furan–maleimide DA reaction. To do so, KL was selectively modified at its phenolic chain ends with furfuryl glycidyl ether (FGE) or 6-maleimidohexanoic acid (6-MHA), to expose pendant furan and maleimide groups, respectively. The functionalizations were monitored by a set of spectroscopic (^{31}P and ^{1}H NMR, UV and FTIR) and chromatographic (SEC) techniques. Finally, furan- and maleimide-grafted lignins were combined in order to perform the DA forward reaction and generate lignin-based gels, which reversibly turned back into the liquid state on performing the retro-DA reaction.

Experimental part

Materials

Softwood Kraft lignin (KL) was obtained from the Lignoboost process.[30] Furfuryl glycidyl ether (FGE, 96%), 6-maleimidohexanoic acid (6-MHA, 90%) and oxalyl chloride were purchased from Sigma-Aldrich and used as received. *N*,*N*-Dimethylformamide (DMF, 99.8%, Sigma-Aldrich) was pre-dried over 4 Å molecular sieves, distilled under vacuum and stored over 4 Å molecular sieves. Dichloromethane (DCM, puriss. p.a., Sigma-Aldrich) was refluxed over $CaCl_2$ for 12 h, distilled off and stored over 4 Å molecular sieves.

Lignin functionalization with furan moieties

KL (500 mg) was dissolved in water containing NaOH (100 mg, 2.5 mmol, corresponding to 1 eq. of total acidic groups in KL, *i.e.* phenolic OH and COOH). After 1 h of stirring, furfuryl glycidyl ether (FGE) was added (from 0.25 to 1.5 eq. of KL phenolic OH) and the reaction mixture was stirred at 50 °C overnight. After cooling to room temperature and acidifying to pH 2 using 10% (v/v) aqueous HCl, the suspension was centrifuged to recover the precipitated lignin. The functionalized lignin was then washed 3 times with 50 mL acidified water (pH 2) and subsequently freeze-dried.

Lignin functionalization with maleimide moieties

6-Maleimidohexanoic acid (6-MHA) was first converted into the corresponding acyl chloride *via* a reaction with oxalyl chloride: 6-MHA (0.5–2.5 eq. of KL phenolic OH) was dissolved in DCM (2.5 mL). Oxalyl chloride (1 eq. of 6-MHA) was added and the reaction was conducted at room temperature under an inert atmosphere for 2 h. Gaseous by-products (HCl, CO and CO_2) were allowed to escape the reaction mixture, and the resulting acyl chloride was used without further purification.

KL (500 mg) was dissolved in dry DMF containing pulverized K_2CO_3 (347 mg, 2.5 mmol, corresponding to 1 eq. of total acidic groups in KL, *i.e.* phenolic OH and COOH). After 1 h of stirring, the solution of acyl chloride in DCM was added dropwise and the reaction mixture was stirred at 50 °C for 1 h, thus allowing the DCM to evaporate.

After cooling to room temperature, 10 mL of water were added and the solution was acidified to pH 6 using 10% (v/v) aqueous HCl, thus allowing the functionalized lignin to precipitate. The suspension was centrifuged to recover the precipitated lignin, and the functionalized lignin was washed 3 times with 50 mL water (adjusted to pH6) before being freeze-dried.

^{31}P NMR

An accurately weighed amount of lignin (about 30 mg) was dissolved in 400 μL of anhydrous $CDCl_3$/pyridine solution (1 : 1.6 v/v). 100 μL of a standard solution of cholesterol (0.1 M in anhydrous $CDCl_3$/pyridine solution) containing Cr(III) acetylacetonate as a relaxation agent was then added. Finally, 100 μL of 2-chloro-4,4,5,5-tetramethyl-1,3,2-dioxaphospholane (Cl-TMDP, 95%, Sigma-Aldrich) were added and the mixture was stirred at room temperature for 2 h. The mixture was then transferred into 5 mm NMR tubes and the spectra were recorded on a Bruker 300 MHz spectrophotometer (256 scans at 20 °C). All chemical shifts reported are relative to the reaction product of water with Cl-TMDP, which gives a sharp signal in pyridine/$CDCl_3$ at 132.2 ppm. Quantitative analysis was performed based on previous literature reports.[31]

^{1}H NMR

An accurately weighed amount of lignin (about 20 mg) was dissolved in 500 μL of DMSO-d_6. 100 μL of a standard solution of 2,3,4,5,6-pentafluorobenzaldehyde in DMSO-d_6 were then added, and the mixture was transferred into 5 mm NMR tubes. The spectra were acquired on a Bruker 300 MHz spectrometer (64 scans at 20 °C).

FTIR

FTIR spectra were recorded on a Perkin Elmer Spectrum 100 FTIR spectrometer. The spectra were acquired on KBr pellets as the average of 32 scans between 450 and 4000 cm^{-1} with a resolution of 4 cm^{-1}.

Phenolic content by UV spectroscopy

The phenolic content of the lignins was measured according to a previously reported UV method, which is based on the difference between the absorption of the phenolic moieties in neutral solution and that of the corresponding phenolate anions in alkaline environments.[32,33] Spectra were recorded between 200 and 400 nm on a Shimadzu UV-1800 spectrophotometer.

Size-exclusion chromatography (SEC)

Prior to SEC, the lignin samples were acetobrominated as reported elsewhere to ensure complete solubilization in THF.[34] Briefly, 5 mg lignin was suspended in 1 mL glacial acetic acid/acetyl bromide (9 : 1 v/v) for 2 h. The solvent was then removed under reduced pressure, and the residue was dissolved in HPLC-grade THF and filtered over a 0.45 μm syringe filter. SEC analyses were performed using a Shimadzu instrument consisting of a controller unit (CBM-20A), a pumping unit (LC 20AT), a degasser (DGU-20A3), a column oven (CTO-20AC), a diode array detector (SPD-M20A), and a refractive index detector (RID-10A). Three analytical GPC columns (each 7.5 × 30 mm) were connected in series for analyses: Agilent PLgel 5 μm 10 000 Å, followed by Agilent PLgel 5 μm 1000 Å and Agilent PLgel 5 μm 500 Å. HPLC-grade THF (Chromasolv®, Sigma-Aldrich) was used as the eluent (0.75 mL min^{-1}, at 40 °C). Standard calibration was performed with polystyrene standards (Sigma Aldrich, MW range 162–5 × 10^6 g mol^{-1}). Final analyses of each sample were performed using the intensities of the UV signal at λ = 280 nm, employing a tailor-made MS-Excel-based table calculation.

Diels–Alder (DA) reactions

The functionalized lignins were dissolved in DMSO at a concentration of 15% (w/w), and heated in an oven at 70 °C without stirring. When gelation occurred, the samples were further heated to 120 °C in an oil bath to perform the retro-DA reaction.

Results and discussion

Lignin functionalization with furan moieties

KL was functionalized with furfuryl glycidyl ether (FGE) to expose furan rings at the phenolic chain end, as depicted in Scheme 1. The reaction was carried out in water containing a stoichiometric amount of NaOH with respect to the total acidic groups in lignin (*i.e.* both COOH and phenolic OH groups). This way, only carboxyl and phenolic OH groups are deprotonated, whereas aliphatic OH groups remain unaffected because of their much higher pK_a. Hence, phenolate ions are the only reactive species, whereas acids are inactivated as carboxylates. Increasing amounts of FGE have been tested, from 0 to 1.5 molar equivalents of lignin phenolic OH groups. The content of functional groups of the derivatized lignins has been monitored using ^{31}P NMR, ^{1}H NMR and UV spectroscopy. All results are listed in Table 1.

The contents of phenolic OH groups measured by ^{31}P NMR and UV spectroscopy are similar (Table 1 and Fig. 1a). All the ^{31}P NMR spectra are available as ESI (Fig. S1†). The depletion of phenolic OH groups follows the stoichiometry of FGE used for the functionalization, indicating a good selectivity. The reaction is indeed quantitative for 1.5 eq. of FGE, since no more phenolic OH groups can be detected. As can be seen in Fig. 1b, the conversion of C5-condensed phenolic groups seems to be slightly

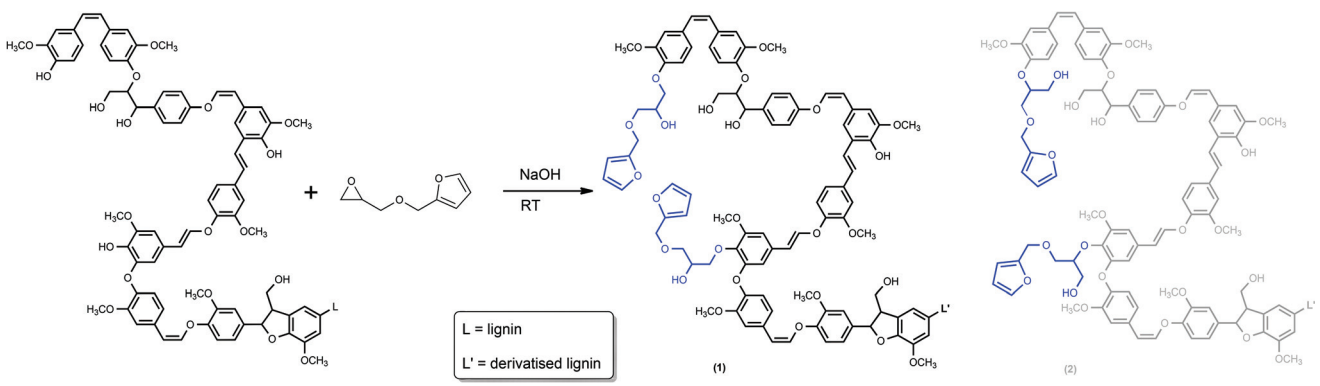

Scheme 1 Reaction of lignin with furfuryl glycidyl ether (FGE). (1) and (2) are the possible products. Only the furfurylated lignin (1) is actually formed under the reaction conditions.

Table 1 Quantification of the functional groups in the lignins derivatized with FGE by UV, ^{31}P and ^{1}H NMR (mmol g^{-1})

		By ^{31}P NMR[a]					By UV[b]	By ^{1}H NMR[c]
Sample name	FGE eq.	Al–OH	Cond. Ph–OH	Uncond. Ph–OH	Total Ph–OH	COOH	Total Ph–OH	Furan
Initial	—	2.00	2.14	2.47	4.61	0.51	3.20 ± 0.10	—
KL_FGE0	0	1.47	1.50	1.52	3.02	0.40	2.86 ± 0.04	—
KL_FGE0.25	0.25	2.35	1.02	0.99	2.01	0.44	1.66 ± 0.02	0.53 ± 0.05
KL_FGE0.5	0.5	2.71	0.62	0.44	1.06	0.41	1.05 ± 0.06	1.07 ± 0.04
KL_FGE0.75	0.75	3.05	0.43	0.25	0.67	0.35	0.61 ± 0.12	1.89 ± 0.09
KL_FGE1	1	3.27	0.29	0.11	0.40	0.30	0.34 ± 0.02	2.03 ± 0.08
KL_FGE1.25	1.25	3.48	0.23	0.09	0.32	0.34	0.18 ± 0.12	2.62 ± 0.11
KL_FGE1.5	1.5	3.29	0.14	0.04	0.19	0.29	0.09 ± 0.01	2.36 ± 0.08

[a] Spectra are available as ESI (Fig. S1). [b] Averages and standard deviations of 3 measurements. [c] Averages and standard deviations of the integrations of the regions 6.2–6.5 ppm and 7.4–7.7 ppm. Spectra are available as ESI (Fig. S2).

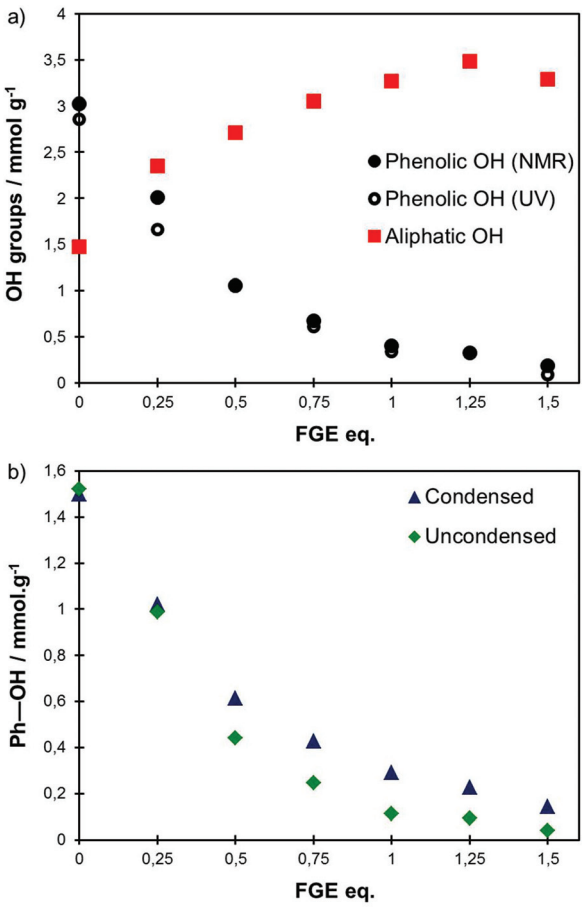

Fig. 1 Content of phenolic and aliphatic OH groups of the lignins functionalized with increasing the amount of FGE (a) and evolution of the content of condensed and uncondensed phenolic OH groups (b).

harder to achieve, most likely because of steric hindrance. A close look at the spectra reveals that the 5–5 condensed structures, giving rise to a signal in the region 140.2–141.7 ppm,[35] are the most recalcitrant to the functionalization (Fig. S1†).

As shown in Scheme 1, the opening of the epoxide produces a new aliphatic OH, thus explaining the increase in the aliphatic OH content (Fig. 1a). It gives rise to a new peak in the ^{31}P NMR spectra at 146.3 ppm, which is distinct from the lignin aliphatic OH signal, as previously observed for a similar reaction with propylene oxide.[36] The regiochemistry of the reaction could not be evaluated by the previously used method, because primary and secondary aliphatic OH group signals overlap. Selected samples were then phosphitylated with 2-chloro-1,3,2-dioxaphospholane and subjected to ^{31}P NMR, since this reagent allows a better resolution of aliphatic OH groups.[37] The corresponding spectra are given as ESI (Fig. S2†). They show the emergence of a new peak in the characteristic region for secondary aliphatic OH groups, at 134.5 ppm, whereas the content of primary aliphatic OH groups remains constant. The increase in secondary aliphatic OH thus measured coincides with the global increase presented in Fig. 1a, within a 5% error margin. This indicates that this reaction proceeds with a high regioselectivity, yielding only compound (1), which is expected to be the favored product resulting from the nucleophilic attack of the C–O bond by the phenolate anion at the less hindered position.

The decrease in phenolic OH is linearly correlated with the increase in aliphatic OH (Fig. 2a). Indeed, the formation of the

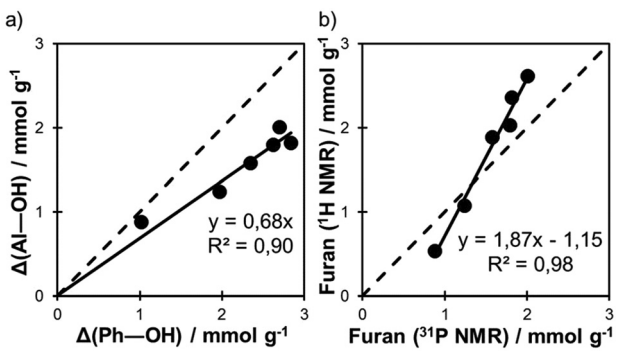

Fig. 2 Correlation between the decrease in phenolic OH (Δ(Ph–OH)) and the increase in aliphatic OH (Δ(Al–OH)), as measured by ^{31}P NMR (a), and correlation between the amount of linked furan groups as measured by ^{31}P and ^{1}H NMR (b).

phenyl ether bond goes along with the generation of a new aliphatic OH group as a result of the epoxy ring opening (Scheme 1). Nevertheless, since data are expressed in mmol g^{-1}, the correlation does not follow a 1 : 1 ratio, because of the increase in molecular weight associated with the FGE introduction. The apparent decrease in phenolic OH groups is thus more important than the concomitant increase in aliphatic OH.

The degree of lignin functionalization, expressed as the loading in furan groups, was evaluated by ^{1}H NMR. The ^{1}H NMR spectra of the functionalized lignins, given as ESI (Fig. S3†), show two new peaks at 6.42 and 7.62 ppm, which are assigned to the H atoms from the furan ring. Those peaks have been integrated in order to calculate the amount of furan groups bound to the lignin. The values obtained from the ^{1}H NMR are compared in Fig. 2b to the corresponding data obtained by ^{31}P NMR, for which the increase in aliphatic OH groups has been taken as representative of the furan loading. A good linear correlation is observed, which however deviates from the $y = x$ curve. The discrepancy can arise from the overlap of the furan signals in ^{1}H NMR with the aromatic protons from lignin.

The molecular weight distributions (MWD) of the functionalized lignins are presented in Fig. 3. The inset shows the progressive increase of the number-average MW, M_n, with the amount of FGE used. The increase is, as expected, quite low, and the differences between the MWD are rather small. Additional difficulties in discussing the magnitude of the MW increase arise from the fact that the samples are acetobrominated prior to SEC analysis, to allow the dissolution in THF. In case the functionalization with FGE is incomplete, the remaining phenolic OH groups are thus converted into acetyls, thus reducing the difference in MW with those functionalized with FGE and minimizing the MW increase caused by FGE.

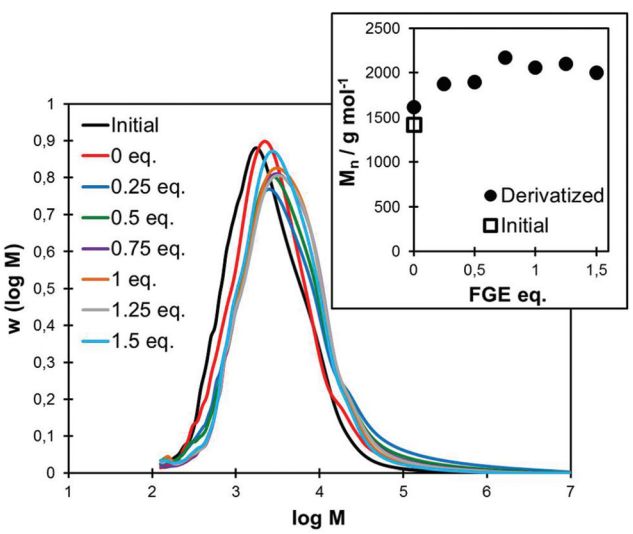

Fig. 3 Molecular weight distributions of the lignins functionalized with 0–1.5 eq. FGE. The inset shows the evolution of M_n with the amount of FGE used for functionalization.

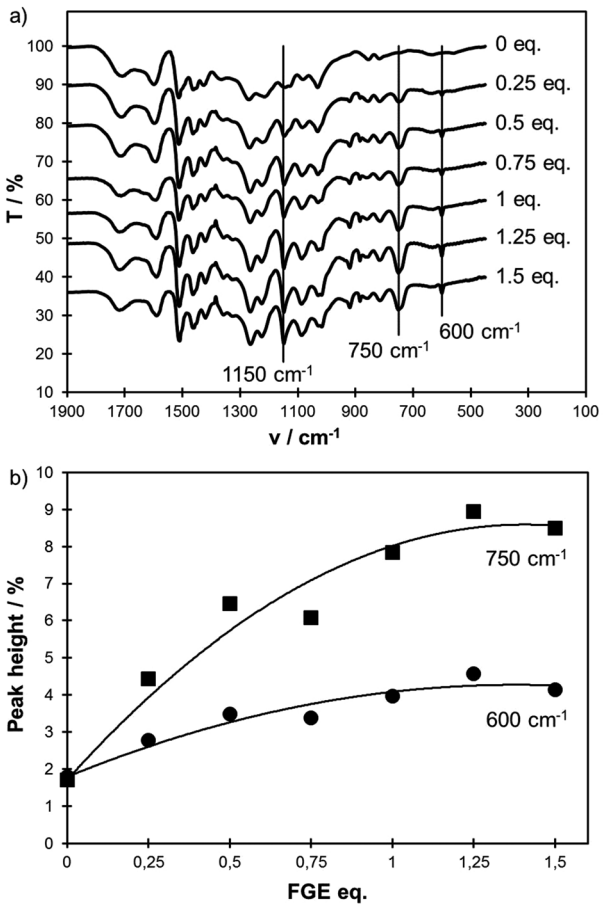

Fig. 4 FTIR spectra of the functionalized lignins, depending on the amount of FGE used for functionalization (a) and evolution of the furan peak heights with the amount of FGE used for functionalization (b).

Further characterization of the functionalized lignins was carried out by FTIR. The spectra recorded for all the samples are shown in Fig. 4a. The main lignin peaks, such as the aromatic skeleton vibration at 1510 and 1600 cm^{-1},[38] are visible on all the functionalized samples. In addition, new peaks characteristic of the furan ring appear in the fingerprint region, at 600 and 750 cm^{-1}. Their intensity correlates well with the amount of FGE used for the functionalization (Fig. 4b). The FTIR data hint at a levelling off when more than 1.25 eq. FGE are used, in good agreement with the data from ^{31}P and ^{1}H NMR. A peak at 1150 cm^{-1}, assigned to the ether bonds in FGE, is also clearly discernible, though it overlaps with other lignin peaks and can thus not be used for quantifying purposes.

Lignin functionalization with maleimide moieties

The second step of the work consisted in the grafting of maleimide groups onto lignin. This was accomplished by esterification with 6-maleimidohexanoic acid (6-MHA), as shown in Scheme 2.

In order to increase the reaction yield, 6-MHA was first converted into the corresponding acyl chloride by reacting with

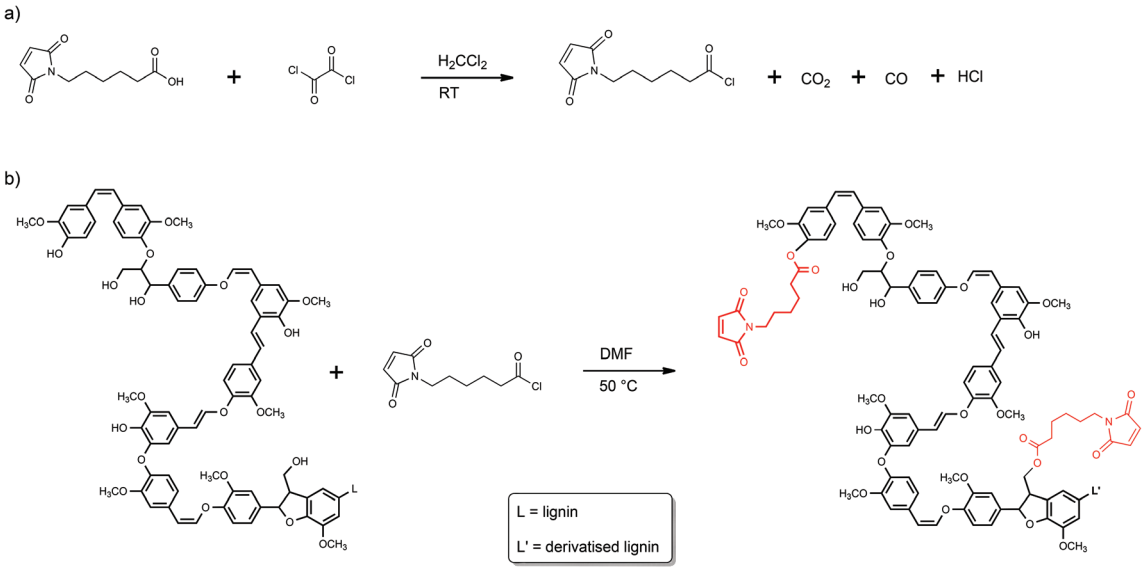

Scheme 2 2-Step maleimidation of lignin: conversion of 6-maleimidohexanoic acid (6-MHA) into the corresponding acyl chloride (a) and esterification of lignin with 6-maleimidohexanoic acyl chloride (b).

oxalyl chloride (Scheme 2a). The solution of acyl chloride was then directly transferred into the lignin solution to perform the esterification (Scheme 2b). The reaction has been performed with increasing amounts of 6-MHA followed by ^{31}P NMR, ^{1}H NMR and UV spectroscopy. All data are given in Table 2.

A preliminary study on the kinetics of the reaction showed that 1 h was sufficient to achieve the maximum functionalization yield (ESI, Fig. S4†). The content of OH groups was measured by ^{31}P NMR, whereas UV spectroscopy was used to monitor the content of phenolic OH groups. Some samples could not be analyzed by ^{31}P NMR, because they were insoluble in the solvent mixture after phosphitylation. In this case only the UV data are reported in Fig. 5a. Nevertheless, when both ^{31}P NMR and UV data are available, a good correlation is observed (Table 2). In order to improve the reaction efficiency, larger reagent excess has to be used to reach a high degree of functionalization, which however does not lead to a complete depletion of phenolic OH groups, since a plateau is observed above 2 eq. 6-MHA.

In addition, a decrease in aliphatic OH groups is also measured, indicating that the esterification does not show selectivity towards phenolic OH groups. The comparison of the reactivity of C5-condensed and non-condensed phenolic units reveals practically no difference at high loading, indicating that the limitation of the reactivity is not caused by steric hindrance.

^{31}P NMR spectra of the functionalized lignins show a strong new peak in the carboxylic acid region at 134.7 ppm (ESI, Fig. S5†). Even if it could in principle arise from unreacted 6-MHA that survived during the workup, the MWD presented in Fig. 6 do not show any additional peak in the low

Table 2 Quantification of the functional groups in the lignins derivatized with 6-MHA by UV and ^{31}P NMR (mmol g^{-1})

		By ^{31}P NMR[a]					By UV[b]	By ^{1}H NMR[c]	
Sample name	6-MHA eq.	Al–OH	Cond. Ph–OH	Uncond. Ph–OH	Total Ph–OH	COOH	Total Ph–OH	6-MHA aliphatic chain	Δ(COOH)
Initial	—	2.00	2.14	2.47	4.61	0.51	3.20 ± 0.10	—	—
KL_6-MHA0	0	1.40	1.45	1.50	2.95	0.28		—	—
KL_6-MHA0.5	0.5	na[d]	na	na	na	na	2.24 ± 0.03	1.33 ± 0.43	0
KL_6-MHA1	1	0.96	1.28	1.50	2.78	0.59	2.29 ± 0.01	1.50 ± 0.24	0.06
KL_6-MHA1.2	1.2	0.86	0.93	1.11	2.04	0.65	2.11 ± 0.05	na	na
KL_6-MHA1.5	1.5	na	na	na	na	na	1.65 ± 0.04	2.39 ± 0.96	0
KL_6-MHA2	2	0.50	0.50	0.55	1.04	1.89	1.27 ± 0.02	2.91 ± 0.51	0.59
KL_6-MHA2.5	2.5	0.51	0.55	0.60	1.15	1.93	1.35 ± 0.05	3.07 ± 0.38	1.18

[a] Spectra are available as ESI (Fig. S5). [b] Averages and standard deviations of 3 measurements. [c] Spectra are available as ESI (Fig. S6). [d] na = not analyzed, because of the insolubility in the ^{31}P NMR solvent mixture after the phosphorylation reaction.

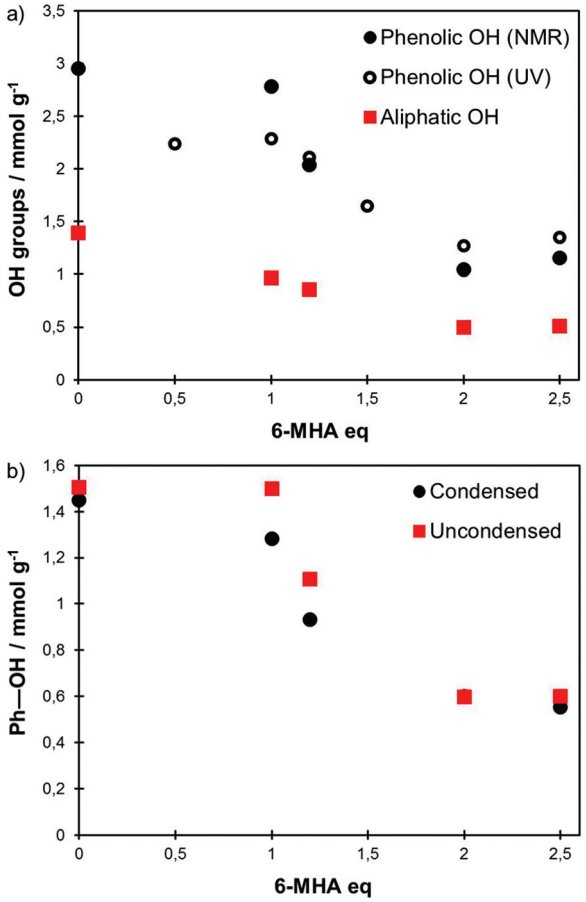

Fig. 5 Content of phenolic and aliphatic OH groups of the lignins functionalized with increasing the amount of 6-MHA (a) and evolution of the content of condensed and uncondensed phenolic OH groups (b).

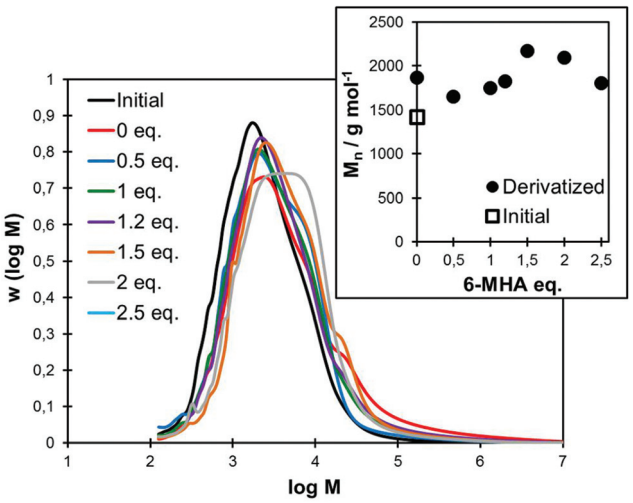

Fig. 6 Molecular weight distributions of the lignins functionalized with 0–2.5 eq. 6-MHA. The inset shows the evolution of M_n with the amount of 6-MHA used for functionalization.

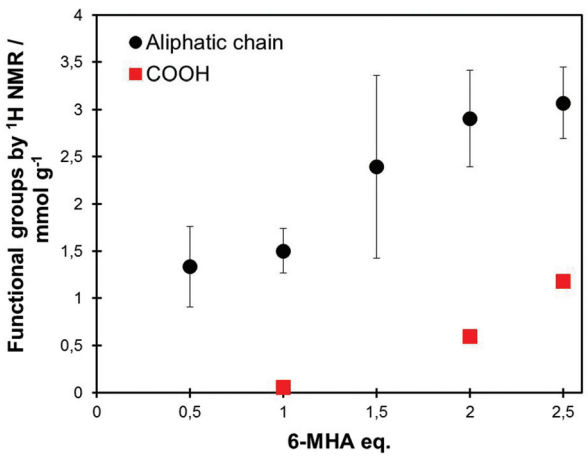

Fig. 7 Functional groups calculated from ^{1}H NMR. Spectra are available as ESI (Fig. S6†). The aliphatic chain has been calculated as the average of the integration regions 2.10–2.30 ppm (^{2}H) and 1.00–1.80 ppm (^{6}H).

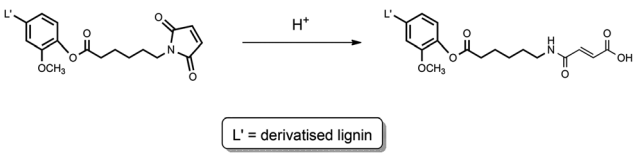

Scheme 3 Possible opening of the maleimide ring under the acidic conditions of the phosphitylation reaction, causing the observed increase in carboxyl groups by ^{31}P NMR.

molecular weight region (M = 211 g mol^{-1} for 6-MHA), despite the absorption of the maleimide group at the detection wavelength (280 nm). On the other hand, ^{1}H NMR spectra, presented as ESI (Fig. S6†), only show a slight increase in the carboxylic acid peak located around 12 ppm. The new COOH groups, calculated from the integration of the ^{1}H NMR spectra, are presented in Fig. 7. The increase is significant only for the samples functionalized with more than 2 eq. 6-MHA, but is always much lower than the one measured by ^{31}P NMR (Table 2). It is thus hypothesized that new carboxyl groups are formed during the phosphitylation reaction necessary for acquiring the ^{31}P NMR spectra. Particularly, acidic conditions during the reaction could lead to the opening of the maleimide ring, which in the presence of residual water could form a new carboxyl group as the chain end (Scheme 3).

The observation of the ^{1}H NMR spectra reveals the appearance of a strong new peak at 7.00 ppm, assigned to the two H atoms of the maleimide ring (Fig. S6†). However, since it overlaps with the aromatic protons of lignin, a precise quantification is impossible. The H atoms from the aliphatic chain of 6-MHA are on the other hand well separated from the lignin protons, and have thus been used to quantify the amount of 6-MHA grafted to the lignin. The results given in Fig. 7 correlate fairly well with the decrease in OH groups obtained from ^{31}P NMR.

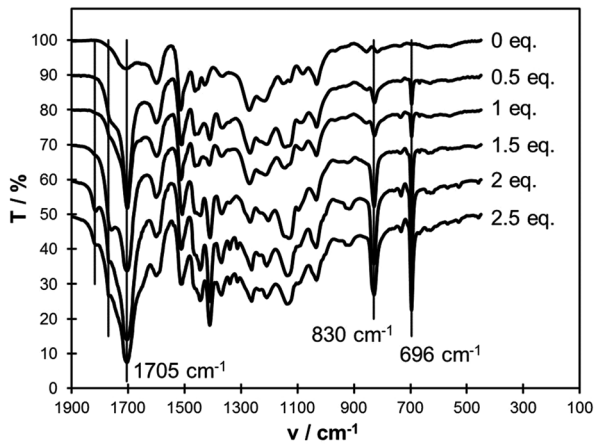

Fig. 8 FTIR spectra of the functionalized lignins, depending on the amount of 6-MHA used for functionalization.

The MWD of the maleimide-functionalized lignins (Fig. 6) show an increase in M_n for the reaction with up to 2 eq. of 6-MHA. The decrease for 2.5 eq. could be related to an incomplete attachment of the 6-MHA, as shown by the increase in COOH groups measured by ^{1}H NMR.

The functionalization of lignin with maleimide groups can also be revealed by FTIR, as shown in Fig. 8. Specific peaks from the maleimide ring appear in the fingerprint region, at 696 and 830 cm^{-1}. The carbonyl region is also strongly enhanced because of numerous contributions. The two C=O groups from the maleimide ring give rise to the signal at 1705 cm^{-1}. The formation of the ester bond between lignin and 6-MHA should be responsible for the shoulder observed around 1770 cm^{-1}.

Reversibly crosslinking lignin *via* the furan–maleimide Diels–Alder (DA) reaction

Once the lignins modified with furan and maleimide groups were prepared, the emphasis was placed on the Diels–Alder (DA) reaction, depicted in Scheme 4. The forward reaction, *i.e.* the crosslinking reaction, was performed at 70 °C, while the retro reaction was conducted at 120 °C.

Samples with similar loading factors in furan (KL_FGE1.25) and maleimide (KL_6-MHA2) were thus mixed in DMSO. The contents of furan and maleimide were respectively 2.31 ± 0.30 and 2.48 ± 0.16 mmol g^{-1}, as evaluated by the averages and standard deviations of the loadings measured by ^{31}P and ^{1}H NMR. An array of experiments was carried out including different ratios of functionalized lignins and control experiments on the initial lignin or on the furan– and maleimide–lignins alone, as shown in Table 3.

In order to study the influence of the concentration, the FGE_MHA_1 : 1 sample was prepared at concentrations from 1 to 15% (w/w). After 4 days at 70 °C, the 15% solution had turned into a gel as a result of the crosslinking, whereas the 10% solution became very viscous and stuck to the walls, as shown in Fig. 9a. No visible change was observed at lower concentration. Upon heating at 120 °C, the gel quickly turned back into the liquid state, as is visible in Fig. 9b, since the crosslinks are removed *via* the retro-Diels–Alder reaction.

Gelation was shown to occur after 36 h when furan– and maleimide–lignins were combined (Fig. S7†), in 1 : 1 or 1 : 2 (w/w) ratios. After performing the retro reaction at 120 °C, the solutions were cooled to room temperature and the gels were formed again at 70 °C, thus confirming the full reversibility of the crosslinking.

Table 3 Compositions of the mixtures of furan- and maleimide-lignins used for studying the Diels–Alder reaction (15% w/w solutions in DMSO)

Sample name	Initial KL (% w/w)	Furan–lignin (% w/w)	Maleimide–lignin (% w/w)	Gelation
Control_KL	100	0	0	No
Control_FGE	50	50	0	No
Control_MHA	50	0	50	No
FGE_MHA_1 : 2	0	33	66	Yes
FGE_MHA_1 : 1	0	50	50	Yes

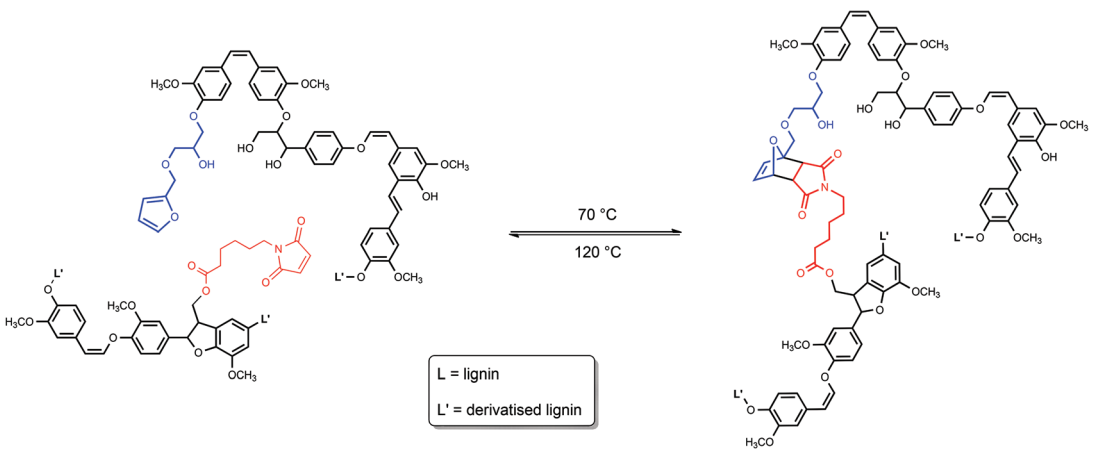

Scheme 4 Crosslinking of the functionalized lignins *via* the Diels–Alder reaction.

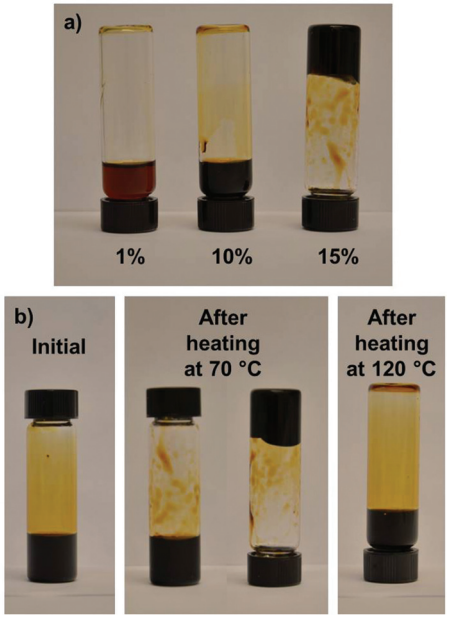

Fig. 9 Solutions of functionalized lignins (furan/maleimide 1 : 1 w/w) in DMSO (1, 10 or 15% w/w) after heating at 70 °C (a) and 15% w/w solution before and after heating at 70 °C and after heating at 120 °C (b).

To assess whether the gelation is related to the formation of the DA adduct between furan and maleimide, similar experiments were performed in DMSO-d_6, followed by acquisition of ^{1}H NMR spectra, reported in Fig. 10. In this case, the concentration was chosen in order not to obtain a gel, which allowed measuring accurate NMR spectra without solubility issues. The signal of the furan protons at 7.62 ppm decreases as the corresponding double bonds are lost during the formation of the DA adducts (Scheme 4). The signal of the maleimide double bond at 7.00 ppm is also reduced, but it overlaps with the lignin aromatic signals, making the quantification difficult. The newly formed double bond of the DA adduct overlaps with the signal of the furan protons at 6.40 ppm. The formation of the DA adduct also generates a new peak at 5.10 ppm, which is clearly discernible in the inset of Fig. 10. After 63 h, the conversion reached 30% as partially expected by the low concentration chosen. It has to be pointed out here that due to the high degree of functionalization of the single lignins the gelation process is expected to occur even with a relatively low conversion of the furan and maleimide groups.

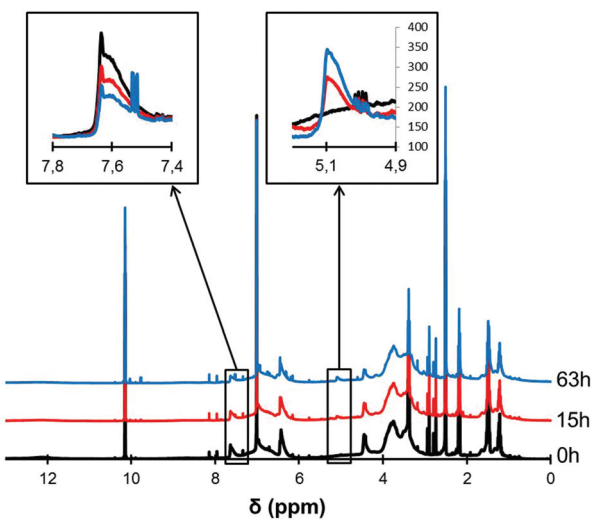

Fig. 10 ^{1}H NMR spectra of F50_M50, recorded after different times at 70 °C.

Conclusion

A synthetic strategy for the specific functionalization of Kraft lignin was developed to obtain furan and maleimide groups respectively linked at the chain ends. The reaction of KL with furfuryl glycidyl ether (FGE) showed a high degree of selectivity towards the phenolic OH groups, and was performed in quantitative yields in the presence of a slight excess of FGE. Maleimide groups were attached by the esterification of KL with 6-maleimidohexanoic acid (6-MHA). With a 2 fold excess of 6-MHA, high loading could be achieved. In this case the reaction was not highly selective, and besides phenolic OH, also some of the aliphatic OH groups of KL were functionalized.

The furan- and maleimide-grafted lignins were then combined to generate a mixture suitable for crosslinking *via* the Diels–Alder (DA) [4 + 2] cycloaddition. The lignin solutions in DMSO turned into a gel at 70 °C as a result of the crosslinking, and quickly turned back into the liquid state after generating the retro-DA reaction at 120 °C. ^{1}H NMR confirmed the formation of the DA adduct, though the conversions were relatively low.

This study thus shows the successful exploitation of the DA reaction to generate reversible crosslinking in lignin. Based on these results, further efforts should now be devoted to the preparation of solid materials, as well as to the study of their properties and potential recyclability or self-healing ability.[39] The developed lignin crosslinking chemistry will be further coupled with other potential applications of lignins, such as the preparation of adhesives, where the thermal reversibility acts as a temporary curing element, in combination with a 'classical' permanent curing system[26] attached to yet unused functional elements present in the lignin, *e.g.*, remaining hydroxyl groups, double bonds, *etc.*

Acknowledgements

The Knut and Alice Wallenberg Foundation is gratefully acknowledged for funding this work.

References

1 G. Gellerstedt and G. Henriksson, in *Monomers, Polymers and Composites from Renewable Resources*, ed. M. N. Belgacem and A. Gandini, Elsevier, Amsterdam, 2008, pp. 201–224.
2 *Handbook of pulp*, ed. H. Sixta, Wiley-VCH Verlag GmbH, 2008.
3 J. Lora, in *Monomers, Polymers and Composites from Renewable Resources*, ed. M. N. Belgacem and A. Gandini, Elsevier, Amsterdam, 2008, pp. 225–241.
4 Z. Strassberger, S. Tanase and G. Rothenberg, *RSC Adv.*, 2014, **4**, 25310–25318.
5 M. P. Pandey and C. S. Kim, *Chem. Eng. Technol.*, 2011, **34**, 29–41.
6 P. Azadi, O. R. Inderwildi, R. Farnood and D. A. King, *Renewable & Sustainable Energy Reviews*, 2013, **21**, 506–523.
7 Z. Strassberger, S. Tanase and G. Rothenberg, *Eur. J. Org. Chem.*, 2011, 5246–5249.
8 Z. Strassberger, A. H. Alberts, M. J. Louwerse, S. Tanase and G. Rothenberg, *Green Chem.*, 2013, **15**, 768–774.
9 J. F. Kadla and H. Chang, *Holzforschung*, 2002, 56.
10 C. Crestini, F. Melone, M. Sette and R. Saladino, *Biomacromolecules*, 2011, **12**, 3928–3935.
11 M. Sette, R. Wechselberger and C. Crestini, *Chem. – Eur. J.*, 2011, **17**, 9529–9535.
12 O. Wallberg, A.-S. Jönsson and R. Wimmerstedt, *Desalination*, 2003, **154**, 187–199.
13 A. Toledano, A. García, I. Mondragon and J. Labidi, *Sep. Purif. Technol.*, 2010, **71**, 38–43.
14 O. Sevastyanova, M. Helander, S. Chowdhury, H. Lange, H. Wedin, L. Zhang, M. Ek, J. F. Kadla, C. Crestini and M. E. Lindström, *J. Appl. Polym. Sci.*, 2014, **131**, 9505–9515.
15 C. Cui, R. Sun and D. S. Argyropoulos, *ACS Sustain. Chem. Eng.*, 2014, **2**, 959–968.
16 A. Duval, F. Vilaplana, M. Lawoko and C. Crestini, *Holzforschung*, 2015, DOI: 10.1515/hf-2014-0346.
17 A. Duval and M. Lawoko, *React. Funct. Polym.*, 2014, **85**, 78–96.
18 Y. S. Kim and J. F. Kadla, *Biomacromolecules*, 2010, **11**, 981–988.
19 I. Dallmeyer, F. Ko and J. F. Kadla, *J. Wood Chem. Technol.*, 2010, **30**, 315–329.
20 C. J. Kloxin, T. F. Scott, B. J. Adzima and C. N. Bowman, *Macromolecules*, 2010, **43**, 2643–2653.
21 G. Tillet, B. Boutevin and B. Ameduri, *Prog. Polym. Sci.*, 2011, **36**, 191–217.
22 H. Nishida, *Polym. J.*, 2011, **43**, 435–447.
23 J. A. Syrett, C. R. Becer and D. M. Haddleton, *Polym. Chem.*, 2010, **1**, 978–987.
24 X. Chen, M. A. Dam, K. Ono, A. Mal, H. Shen, S. R. Nutt, K. Sheran and F. Wudl, *Science*, 2002, **295**, 1698–1702.
25 E. B. Murphy and F. Wudl, *Prog. Polym. Sci.*, 2010, **35**, 223–251.
26 G. J. Berg, T. Gong, C. R. Fenoli and C. N. Bowman, *Macromolecules*, 2014, **47**, 3473–3482.
27 L. Xue, A. Kovalev, K. Dening, A. Eichler-Volf, H. Eickmeier, M. Haase, D. Enke, M. Steinhart and S. N. Gorb, *Nano Lett.*, 2013, **13**, 5541–5548.
28 A. Gandini, *Prog. Polym. Sci.*, 2013, **38**, 1–29.
29 A. Gandini, *Green Chem.*, 2011, **13**, 1061–1083.
30 P. Tomani, *Cellul. Chem. Technol.*, 2010, **44**, 53–58.
31 A. Granata and D. S. Argyropoulos, *J. Agric. Food Chem.*, 1995, **43**, 1538–1544.
32 *Functional Analysis of Lignins and Their Derivatives*, ed. G. F. Zakis, Tappi Press, Atlanta, GA, 1994.
33 A. Gärtner, G. Gellerstedt and T. Tamminen, *Nord. Pulp Pap. Res. J.*, 1999, **14**, 163–170.
34 J. Asikkala, T. Tamminen and D. S. Argyropoulos, *J. Agric. Food Chem.*, 2012, **60**, 8968–8973.
35 B. C. Ahvazi, G. Pageau and D. S. Argyropoulos, *Can. J. Chem.*, 1998, **76**, 506–512.
36 H. Sadeghifar, C. Cui and D. S. Argyropoulos, *Ind. Eng. Chem. Res.*, 2012, **51**, 16713–16720.
37 D. S. Argyropoulos, *J. Wood Chem. Technol.*, 1994, **14**, 45–63.
38 O. Faix, in *Methods in Lignin Chemistry*, ed. S. Y. Lin and C. W. Dence, Springer-Verlag, Berlin-Heidelberg, 1992, pp. 83–109.
39 Y.-L. Liu and T.-W. Chuo, *Polym. Chem.*, 2013, **4**, 2194–2205.